Renewable and Sustainable Energy Reviews 16 (2012) 4563–4573

Contents lists available at SciVerse ScienceDirect

Renewable and Sustainable Energy Reviews

journal homepage: www.elsevier.com/locate/rser

A new strategy for predicting short-term wind speed using soft computing models

Ashraf U. Haque [a], Paras Mandal [b,*], Mary E. Kaye [a], Julian Meng [a], Liuchen Chang [a], Tomonobu Senjyu [c]

[a] Department of Electrical and Computer Engineering, University of New Brunswick, Fredericton, New Brunswick, Canada E3B 5A3
[b] Department of Industrial, Manufacturing and Systems Engineering, University of Texas at El Paso, El Paso, TX 79968, USA
[c] Department of Electrical and Electronics Engineering, University of the Ryukyus, Okinawa 903-0213, Japan

ARTICLE INFO

Article history:
Received 16 March 2012
Received in revised form
23 May 2012
Accepted 26 May 2012
Available online 27 June 2012

Keywords:
Adaptive neuro-fuzzy inference system
Short-term wind speed forecasting
Backpropagation neural network
Radial basis function neural network
Similar days

ABSTRACT

Wind power prediction is a widely used tool for the large-scale integration of intermittent wind-powered generators into power systems. Given the cubic relationship between wind speed and wind power, accurate forecasting of wind speed is imperative for the estimation of future wind power generation output. This paper presents a performance analysis of short-term wind speed prediction techniques based on soft computing models (SCMs) formulated on a backpropagation neural network (BPNN), a radial basis function neural network (RBFNN), and an adaptive neuro-fuzzy inference system (ANFIS). The forecasting performance of the SCMs is augmented by a similar days (SD) method, which considers similar historical weather information corresponding to the forecasting day in order to determine similar wind speed days for processing. The test results demonstrate that all evaluated SCMs incur some level of performance improvement with the addition of SD pre-processing. As an example, the SD+ANFIS model can provide up to 48% improvement in forecasting accuracy when compared to the individual ANFIS model alone.

Contents

1. Introduction

Wind energy is considered as one of the fastest growing energy resources in the world. Globally, wind energy saw an average annual growth rate of 31% over the past five years. By 2020, 12% of the world's electricity could feasibly come from wind power. Wind represents a clean and sustainable source of energy and is in abundant supply. However, the increase in wind power

* Corresponding author. Tel.: +1 915 747 8653; fax: +1 915 747 7184.
E-mail addresses: ashraf.haque@unb.ca (A.U. Haque), pmandal@utep.edu (P. Mandal), kaye@unb.ca (M.E. Kaye), jmeng@unb.ca (J. Meng), lchang@unb.ca (L. Chang), b985542@tec.u-ryukyu.ac.jp (T. Senjyu).

1364-0321/$ - see front matter © 2012 Elsevier Ltd. All rights reserved.
http://dx.doi.org/10.1016/j.rser.2012.05.042

penetration requires a number of issues to be addressed including the management of wind power generation variability, market integration, interconnection standards, power quality, power system stability and reliability, etc., and as such, the power grid operators and energy traders face a number of challenges due to the substantial growth of increased wind power penetration in electricity energy systems [1,2]. Since the wind power produced by a wind farm depends critically on the stochastic nature of wind speed, unexpected variations of a wind power output may increase operating costs for the electricity system.

The relationship between wind speed and wind power is highly nonlinear (i.e., basically cubic), hence, any error in the wind speed forecast will actually generate a larger error in wind power production. When an entire wind farm is considered, the relationship becomes more complex as speed and directional components of the wind are used by individual turbines to achieve an optimal power output of the wind farm [3]. Correspondingly, the application of short-term wind speed forecasting (30-min to 6-h-ahead) is instrumental in the planning of economic load dispatch and load increment/decrement decisions making with respect to the management of a significant amount of wind power.

Several methods are reported in the literature for short-term wind speed forecasting such as the persistence method, physical modeling approaches, time-series techniques, soft computing methods, etc. The persistence method, also known as a 'Naive Predictor', is generally used as a benchmark for comparing other tools for short-term wind speed forecasting. This method simply uses the past hour wind speed value as the forecast for the next hour. Wind forecasting methods are usually first tested against the persistence method in order to baseline its performance [3]. Numerical weather prediction (NWP) is a physical modeling approach used in forecasting wind that utilizes various weather data and operates by solving complex mathematical models [4,5]. Also, a number of time-series forecasting models have been successfully applied to short-term wind speed forecasting. The time-series based model uses historical data to tune the model parameters and error minimization occurs when the patterns match historical ones. Some examples of time-series models are autoregressive moving average (ARMA), autoregressive integrated moving average (ARIMA), fractional ARIMA (fARIMA), seasonal ARIMA (sARIMA), single exponential technique, double exponential, grey predictors [3,6–10]. These time-series models perform well in the areas where the data is low frequency in nature such as weekly patterns, but can have difficulties when there are rapid variations and high-frequency changes of the target signal, e.g., wind speed. Furthermore, wind speed is a result of the complex interactions between large-scale forcing mechanism, e.g., pressure and temperature gradients, rotation of the earth and local characteristics of the surface. These attributes make accurate wind speed forecasting more difficult and highly model dependent.

Soft computing methods are well known for their capabilities when dealing with non-linear systems and have garnered significant attention in the area of wind forecasting. Soft computing is a generalized term that encompasses the fields of neural networks (NNs), fuzzy logic, evolutionary computation, machine learning and probability reasoning. An advantage of the soft computing model (SCM) is its lower data dependency compared to statistical models and can also handle data non-linearity more effectively [11,12]. Another advantage of SCMs is that they do not require a priori knowledge of the wind data model [13]. However, drawbacks of SCMs include the inherent implicit or hidden input/output data relationship and the possibility of overly excessive computational requirements [10]. Among SCMs, NNs have been widely used in various forecasting applications and numerous types of NNs including backpropagation NN (BPNN), probabilistic NN, radial basis function NN (RBFNN), self-organizing feature maps (SOFM), cascade correlation NN, extended Kalman filter (EKF)-based NN, support vector machine (SVM), and adaptive resonance theory NN have been previously suggested [14–17]. Some evolutionary optimization techniques, e.g., particle swarm optimization (PSO), genetic algorithms (GA) have been used for updating the weight of a neuron while training the NN [18]. Also, fuzzy theory has been used for various forecasting applications [19,20] and another approach for short-term wind speed forecasting based on the fuzzy ARTMAP technique was explored in [21].

Approaches using a hybrid intelligent system for wind speed forecasting are becoming more popular, namely neuro-fuzzy methods. Fuzzy logic and NNs are natural complementary tools. A wide comparison among ARMA, NNs, and adaptive neuro-fuzzy inference system (ANFIS) models are presented in [22] for forecasting wind power in five forecasting horizons (1 h, 3 h, 6 h, 12 h, and 24 h). Li et al. [23] proposed the use of a Bayesian combination method using NN models and showed improved wind speed forecasting accuracy. Cadenas and Rivera [24] used a hybrid ARIMA-NN model for wind speed forecasting and their results demonstrated that the forecasting performance of this hybrid model for a fixed prediction horizon was significantly better compared to that of the ARIMA and the NN models working separately. Blonbou [25] presented an adaptive very short-term wind power prediction scheme using NNs as predictor along with adaptive Bayesian learning and Gaussian process approximation. The results showed that the NN predictor performs better than the persistence model and the Bayesian framework permits the prediction of the interval within which the generated power should be observed. Recently, Bhaskar and Singh [26] applied an adaptive wavelet neural network (AWNN) based wind speed forecast model and utilizes multiresolution decomposition of wind speed signal. It was found that the AWNN model has better forecasting accuracy and a faster training ability when compared to a conventional feed forward neural network (FFNN). Given the wide variations of wind forecasting algorithms, a standardized protocol for evaluating short-term wind power prediction systems was introduced in [27,28] where the authors also provided guidelines for using a minimum set of error measures. It was emphasized that a rigorous use of data is required as well as the fact that both training and testing data sets should be clearly defined and separated. Giebel et al. [29] presented a literature overview on the state-of-the-art in short-term wind power prediction. The authors stated that wind power prediction tool is not "plug-and-play" as it highly depends on wind farm site, and when installed to a new site, a considerable effort is needed for tuning the models based on the characteristics of the local wind profile. As explained here, several forecasting methods are available for wind speed forecasting, however, there is still a need of an efficient and robust forecast tool.

This paper describes short-term wind speed forecasting approaches by considering various SCMs, and the combined approach of an SCM and the similar days (SD) method for data pre-processing. The forecasting is applied to data obtained from the North Cape wind farm located in the Prince Edward Island (PEI), Canada. This paper reports the results obtained for 1-h-ahead (case-I) and 3-h-ahead (case-II) wind speed forecasts for the randomly chosen days of multiple seasons of the year 2010. The forecasting horizon in both the cases are 24 h and 72 h. In this paper, the following forecasting procedures are analyzed:

(i) forecasting based on averaging a selected number of similar wind speed days corresponding to forecast day, i.e., SD method.
(ii) forecasting based on considering BPNN only.
(iii) forecasting based on considering RBFNN only.
(iv) forecasting based on considering ANFIS only.

(v) forecasting based on an integrated forecasting model by utilizing SD combined with the SCM where the output of the SD method ($\widehat{SD}$) is fed into the SCM in order to obtain the final estimate of wind speed. In other words, the wind speed forecasts process is based on averaging a selected number of similar wind speed days and refining the results through the application of SCM. Three different models were assessed here: SD+BPNN, SD+RBFNN, and SD+ANFIS.

Hence, there were a total seven different forecasting models: four individual models, namely SD, BPNN, RBFNN, and ANFIS, and three combined models, namely SD+BPNN, SD+RBFNN, and SD+ANFIS that were assessed for wind speed forecasting accuracy. It is emphasized that though the performance of seven different forecasting models are explored in the paper, this paper introduces SD+ANFIS as the proposed short-term wind speed forecasting model. To demonstrate the effectiveness of the proposed hybrid SD+ANFIS model, the proposed model is compared with all other individual and combined models as well as with the methods based on the linear prediction (LP) and NWP. Furthermore, 1-h-ahead forecasting results were also compared with the persistence method, which is considered as a benchmark method. The test results demonstrate a satisfactory forecasting performance of all the hybrid models (SD+BPNN, SD+RBFNN, and SD+ANFIS) considered in this paper, however, a large reduction in forecast error of an individual ANFIS model by more than 40% reflects the effectiveness of the proposed hybrid model based on SD+ANFIS. The forecasting performance of the proposed SD+ANFIS is not only more adequate and effective than the individual forecasting performance of ANFIS, but also it performs better than the single use of SD method, BPNN, RBFNN, LP, NWP as well as the integrated approaches using SD+BPNN and SD+RBFNN models. In general, the test results demonstrate that the proposed SD+ANFIS based prediction model performs effectively in transforming the given numerical weather data into wind speed predictions with a significant reduction in forecasting errors.

The proposed hybrid SD+ANFIS model for wind speed prediction is characterized by:

- SD method based model performs a linear mapping between inputs and outputs. The ANFIS model is a hybrid of two intelligent system models and combines the low-level computational power of an NN with the high-level reasoning capability of a fuzzy system thus providing smoothness and adaptability. Hence, the combination of SD and ANFIS provides a robust approach to wind speed prediction.
- Ability of modeling the interaction of wind speed and other weather parameters such as wind direction and temperature in the forecast process.
- Effective forecasting performance for multiple seasons with higher accuracy.
- The SD method requires a large amount of historical data for modeling the input parameters.
- The ANFIS model has a higher computational complexity. In other words, the learning complexity of this model is highly affected when inputs or membership functions are increased.

While there are several papers discussing the wind speed forecasting topic, the original contribution of this paper is an upgrade of the existing techniques. The fundamental and novel contribution is the choice of some input factors based on SD technique for better accuracy and proposing a new hybrid forecasting technique based on the combination of SD method and SCM(s) in order to translate the practically available numerical weather data from a wind farm into wind speed signals.

The rest of this paper is organized as follows. Section 2 presents wind speed forecasting by SD method. Soft computing models are discussed in Section 3 followed by the numerical results and discussion in Section 4. Section 5 includes the final conclusions of the paper.

2. Similar days method for wind speed forecasting

The basic principle of the SD method is to match historical with similar properties to that of the forecast day [30]. In the context of wind speed similarity, minimum-distance Euclidean criterion is adopted in this paper in order to evaluate the similar wind speed days corresponding to the forecast day.

A proper selection of input variables is important in order to have the better performance of the prediction model. Even though many exogenous variables can have a good relationship with wind speed, it is not feasible or efficient to consider all of them in the forecasting process. Some of the major factors affecting the wind speed (WS) are wind direction (WD), temperature (T), pressure, humidity, etc. This paper considers an interaction between WS and other weather parameters such as WD and T in the wind speed forecast process. Other influential aspects such as humidity, pressure, etc., are not considered as inputs in this paper; however, these aspects will be explored in our future work. For the selection of similar days, the following Euclidean norm equation adopts WS at time t and $t-1$, and wind direction at t.

$$\|EN\| = \sqrt{\widehat{w}_1(\Delta WS_t)^2 + \widehat{w}_2(\Delta WS_{t-1})^2 + \widehat{w}_3(\Delta WD_t)^2}, \quad (1)$$

where

$$\Delta WS_t = WS_t - WS_t^{past}, \quad (2)$$

$$\Delta WS_{t-1} = WS_{t-1} - WS_{t-1}^{past}, \quad (3)$$

$$\Delta WD_t = WD_t - WD_t^{past}, \quad (4)$$

where $\|EN\|$ is Euclidean norm; WS_t and WD_t are WS and WD on the forecast day, respectively. WS_{t-1} is WS at $(t-1)$ on the forecast day. WS_t^{past} and WD_t^{past} are WS and WD in the historical days, respectively. WS_{t-1}^{past} is the WS at $(t-1)$ on the historical days. ΔWS_{t-1} and ΔWD_{t-1} are the WS and WD deviation between the forecast day and the similar days in past, respectively. $\widehat{w}_i$ $(i = 1-3)$ is the weighting factor and it is determined by using the method of least squares [31,32]. Eq. (1) is an important equation for the selection of similar wind speed days based on the historical data. Note that SD represents *similar wind speed days* throughout this paper. We can observe from (1) that an interaction of WS and WD is taken into consideration during the SD selection process. In order to minimize the input variables without compromising the accuracy of the SD based forecasting method, it is observed that WS and WD at the same hour, and WS at the previous hour are appropriate inputs to find the SD. Note that WD is a circular variable. Authors attempted to incorporate circularity effect in (1) and found comparatively worse performance of the SD method with high forecasting error. Literature review also suggest that there is no significant improvement in wind speed prediction when sine and cosine of wind direction is considered [33,34].

Similar days are based on the same season. In Fig. 1, the slanted portion indicates the ‘forecasting period’ and $D*3 = 135$ days is the time framework for the selection of SD corresponding to forecast day, i.e., the SD method considers the previous 45 days (*e.g., as shown in Fig.* 1, *this data goes back till August* 17, 2010) from the day before a forecast day (*September* 30, 2010 at 23:00 h), and 45 days before (*August* 17, 2009) and after (*November*14, 2009) from the forecast day in the previous year (*September*30, 2009 *at*23:00 h) for the selection of similar days. SD method gives hourly calculation.

It means SD method uses $45*3*24 = 3240$ hourly data points. Among these hourly data, the SD method chooses the lowest 100 values from (1) using $\|EN\|$ criterion, i.e., 100 low values are sorted out of 3240. Note that the lower the value of $\|EN\|$, better the selection of SD. Then, these 100 values are averaged in order to get the SD forecast. Authors did sensitivity analysis by choosing various data samples as 10, 20, 30, 50, 75, 100, 150, and 200, and it was found that the data sample with 100 produces the best result. In Fig. 1, September 30, 2010 at 23:00 h is chosen as a forecast day for illustration purposes only. It should be noted that if the forecast day is changed, similar days are selected in the same manner.

An illustration of the selection of hours for the SD criterion is shown in Fig. 2(i) and (ii) where 1-h-ahead and 3-h-ahead forecasting procedures utilizing the SD method are described. For instance, in Fig. 2(ii), similar wind speed data is selected by calculating $\|EN\|$ from (1), i.e., wind speed data of SD at time $t+1$ are obtained first and it is assumed to be the forecasted wind speed $\widehat{SD}_{t+1}$ at time $t+1$. Note that (1) gives an hourly calculation of $\|EN\|$. $\widehat{SD}_{t+1}$ is an average of 100 selected hours of SD data, and using it, SD wind speed forecast $\widehat{SD}_{t+2}$ is obtained for time $t+2$. $\widehat{SD}_{t+2}$ is again an average of 100 selected hours of SD data. In other words, a different set of 100 SD data is selected for each hour based on (1). This process continues until the target hour, i.e, once the forecasted SD data $\widehat{SD}_{t+2}$ is obtained at $t+2$, this SD output is used in order to select similar days wind speed data at $t+3$, i.e., $\widehat{SD}_{t+3}$, thus providing 3-h-ahead SD based wind speed forecasts. For example, in Fig. 2(ii), for calculating $\widehat{SD}_{t+1}$, i.e., WS at 00:00 on 10/01/2010, the input parameters are WS_t, WS_{t-1}, and WD_t, where t is 23:00 on 9/30/2010. To get the value of $\widehat{SD}_{t+2}$, i.e., WS at 01:00 on 10/01/2010, the input parameters are $\widehat{SD}_{t+1}$, WS_t, and WD_{t+1}, where t is 23:00 on 9/30/2010. Similarly, to get the value of $\widehat{SD}_{t+3}$, i.e., WS at 02:00 on 10/01/2010, the input parameters are $\widehat{SD}_{t+2}$, $\widehat{SD}_{t+1}$, and WD_{t+2}, where t is 23:00 on 9/30/2010. Note that the SD calculation considers the available wind direction data for time $t+1$ and $t+2$. In this paper, SD forecasts are then considered as inputs to the SCMs in order to produce the final forecasts. The described procedure for the SD criterion is shown in Fig. 3.

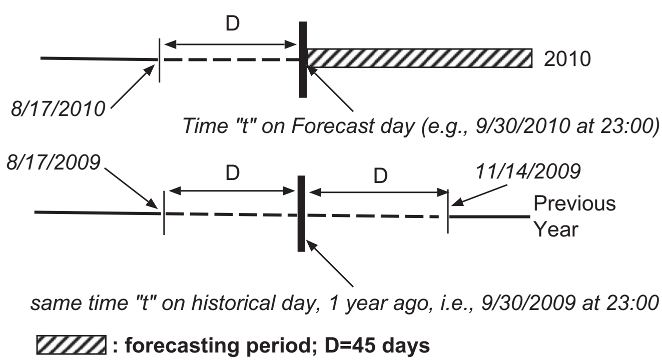


Fig. 1. Evaluation of SD based on historical information.

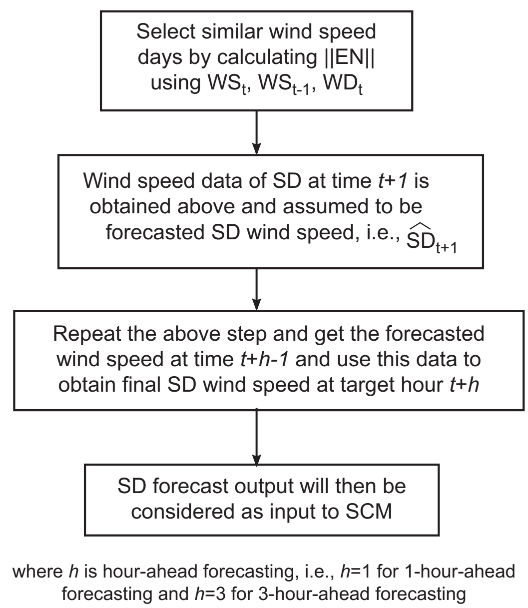


Fig. 3. Forecasting process based on SD method.

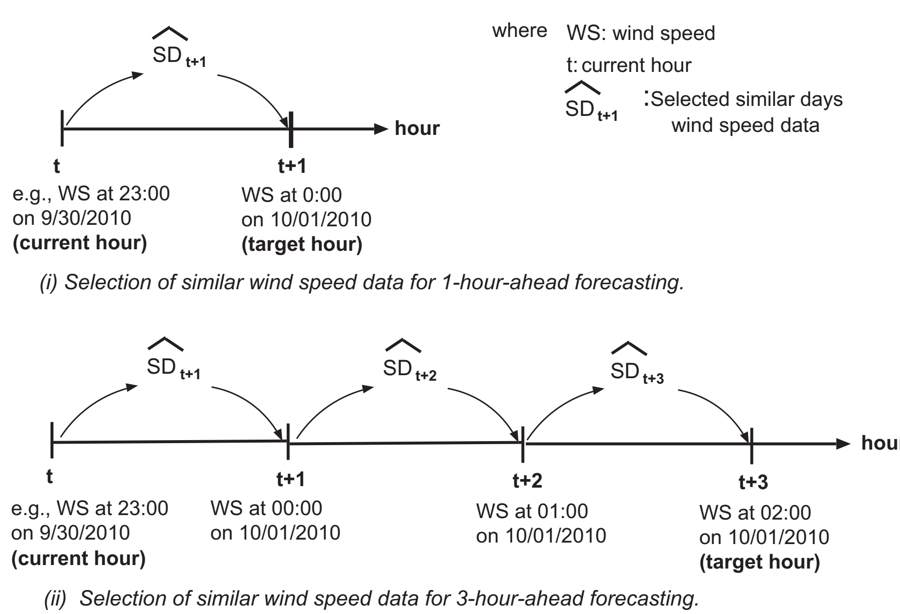


Fig. 2. Illustration of 1-h-ahead and 3-h-ahead SD based wind speed forecast.

3. Soft computing models for wind speed forecasting

Due to their strong learning, cognitive ability and good tolerance to uncertainty, SCMs are suitable for the wind speed forecasting application. In this paper, BPNN, RBFNN and ANFIS are the considered SCMs for wind speed forecasting, and these SCMs are separately combined with the SD method to achieve better forecasting performance.

3.1. Backpropagation neural network

The BPNN is one of the most popular forecasting tools among various SCMs. The network architecture is shown in Fig. 4. The network's weights and biases are the keys to the network's ability to forecast wind speed accurately. In each iteration of the simulation, the weights and biases are adjusted to minimize the error function [35,36]. The interconnectivity among nodes of an NN allows for the ability to learn relationship between input-output pairs. The "learned" relationship between the input and target output is developed during the training phase. The network then obtains the wind forecast output from the test set using the trained network. In this paper, the BPNN is learned by using Levenberg-Marquardt algorithm. The following energy function is used as a stopping criterion during the learning procedure [31,37]:

$$e=\frac{1}{2}\sum(O-O^*)^2, \tag{5}$$

where O and O^* are network output and desired output, respectively.

The three-layered BPNN model, as shown in Fig. 4, considers WS, WD and T at time t, and the SD forecasted values ($\widehat{SD}_{t+1}$, $\widehat{SD}_{t+2}$, $\widehat{SD}_{t+3}$) as inputs. The final forecasts are 3-h-ahead wind speed forecasting. Note that for 1-h-ahead forecasting, the architecture of the BPNN is the same as that of Fig. 4 except that it does not consider $\widehat{SD}_{t+2}$ and $\widehat{SD}_{t+3}$ as inputs.

3.2. Radial basis function neural network

The RBFNN model has a form similar to BPNN. The structure of the RBFNN model is shown in Fig. 5. The hidden layer neurons in RBFNN contain the radial basis function, which differs it from the BPNN, and this paper considers the Gaussian function as a radial basis function. A function is radial basis if its output depends on the distance of the input from a given stored vector [38]. In the RBFNN model, the input is sent to the hidden layer without being weighted and the final layer output is the weighted sum of the hidden layer's outputs without transformation. Input parameters considered in the RBFNN model are similar to that of Fig. 4 in both 1-h-ahead and 3-h-ahead forecasting. The output of the hidden neurons H_m is converted by the radial basis function neuron and is expressed as [39]

$$H_m(x)=f(\phi\|x_i-C_i\|)=\exp((x_i-C_i)^2/\sigma_i^2), \tag{6}$$

where m is hidden neuron and σ is the parameter, which controls the smoothness of the Gaussian function ϕ. x_i is the input vector and C_i refers to the center of point input vector x. Each hidden-unit output is obtained by closeness of the input vector x_i to an n-dimensional parameter vector C_i associated with the ith hidden unit [39]. The output of the hidden layer is multiplied by a weight associated with the neuron and passed to the summation, which adds up the weighted value, and it is denoted by

$$y_i=\sum_{n=1}^{N}(w_nH_m(x)), \tag{7}$$

where w_n denotes the weight associated hidden layer to output layer.

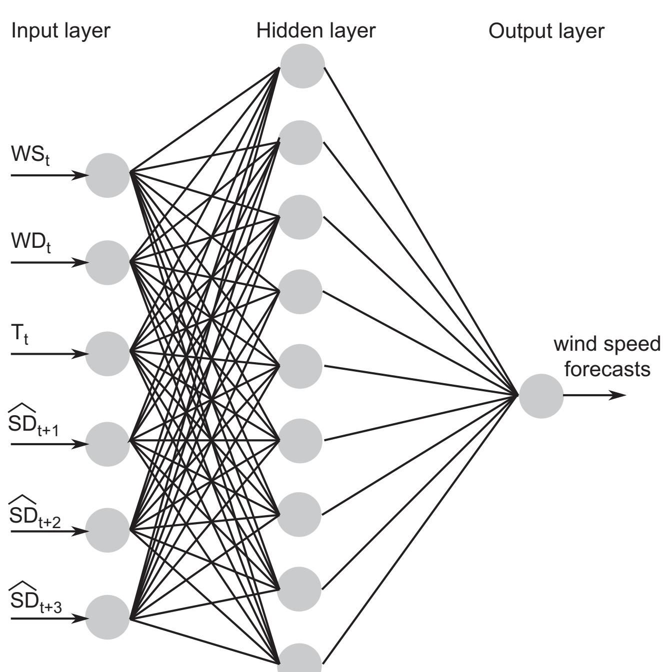


Fig. 4. Architecture of the BPNN model for 3-h-ahead forecasting.

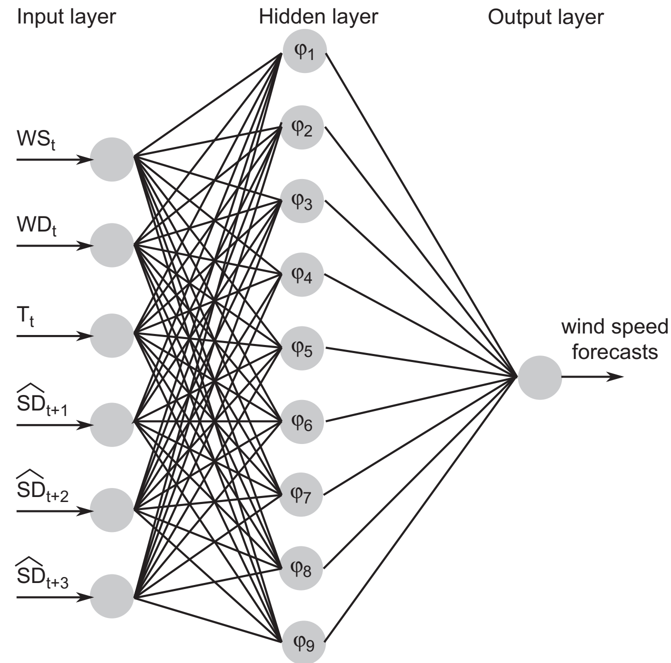


Fig. 5. Architecture of the RBFNN model for 3-h-ahead forecasting.

3.3. Adaptive neuro-fuzzy inference system

The NNs have a low-level computational structure, whereas fuzzy logic deals with reasoning on a higher level. However, the disadvantage of using fuzzy logic is that fuzzy systems are unable to learn and cannot adjust themselves. Hence, a hybrid network based on fuzzy system and NN can be a good strategy to improve short-term wind speed forecasting accuracy [37]. This hybrid system has thus advantages of both neural networks (e.g., learning capabilities, optimization capabilities), and fuzzy systems (e.g., human-like 'if-then' rules, and ease of incorporating expert

knowledge available sometimes in linguistic terms) [40–42]. The five-layered ANFIS model is as shown in Fig. 6. Note that the SD method is combined with ANFIS model making an integrated forecasting model as SD+ANFIS. Among different individual and integrated SCMs implemented in the paper, this paper focuses on the SD+ANFIS technique as the proposed wind speed forecasting model. As shown in Fig. 6, each layer of the ANFIS has its own task, which is briefly described as:

Layer 1 is an input membership function layer. The inputs are fuzzified here. Three membership functions are used, and *A*, *B*, *C*, *D* use bell-shaped membership functions [41].

Layer 2 is a rule layer and the outputs of which represent the membership grade of the corresponding inputs. The node generates the output by cross multiplying all the incoming signals. Each output node represents the firing strength of a rule. If M is the number of the membership function and K is the number of the input, then M^K gives the total number of rules. Given the large number of rules used in this paper, the connection between layer 1 and layer 2, and also between layer 2 and layer 3 are shown partially in Fig. 6.

Each node of the layer 3 receives inputs from all nodes from the layer 2 and calculates the normalized firing strength, which is the ratio of the firing strength of a given rule to the sum of firing strengths of all rules [42].

Layer 4 is the defuzzification layer. Each neuron in this layer is connected to the output of the layer 3 and also connects to all inputs. The output of the layer 4 is the function of consequent parameters of rules created from layer 3 and input variables [37].

Layer 5 is the output layer. The single node in this layer is a fixed node, which computes the overall output by summing all incoming signals and produces wind speed forecasts.

A higher number of inputs or membership functions can produce a large number of fuzzy rules, which can increase the learning complexity. To reduce this complexity, $\widehat{SD}_{t+1}$, $\widehat{SD}_{t+2}$ and $\widehat{SD}_{t+3}$ are averaged, i.e., $\widehat{SD}_{t_1,t_2,t_3}$, and then considered as one of the input parameters along with WS, WD and T at time t (see Fig. 6).

3.4. Training and testing procedure for SCMs

The procedure for the proposed algorithm to forecast *h*-hour-ahead wind speed including learning and forecasting methodology of the SCMs is described below:

Step-1: Get historical WS, WD and T data.

Step-2: Select *h*-hour-ahead (where $h=1$ and 3) and forecasting horizon (24 or 72 h).

Step-3: Select SD for the first learning day of SCM from the time framework for the selection of SD (see Fig. 1), which considers the previous 45 days from the day before a forecast day, and 45 days before and after from the forecast day in the previous year, i.e. $45*3*24=3240$ hourly sample data. Among these hourly data, the SD method chooses the lowest 100 values from Eq. (1) using $\|EN\|$ criterion. Then, 100 selected SD are averaged to get $\widehat{SD}$.

Step-4: Training data of SCM. The online training of the SCM has been adopted in this paper. Past 30 days data from the day before a forecast day are used for training the SCM. Training data includes WS, WD, T, and $\widehat{SD}$ where $\widehat{SD}$ is the SD forecast output.

Step-5: SCM learning algorithm is applied to train the network. The SCM is trained for all the days of learning range (30 days) using WS, WD, T including $\widehat{SD}$ obtained from Step-3. Note that each learning day of the learning range has one learning data set and that makes the total data set of $30*24=720$. Once the training data set reaches the 720th hour of the learning range, this ends the cycle-1, i.e., epoch-1. The stopping criterion is an early stopping with maximum number of iterations as 1000 epochs. Table 1 presents the training parameter of SCMs.

Step-6: The training of the SCM is completed in Step-5. Then, we select the SD wind speed data, which is an average of 100 selected SD data, corresponding to the forecast day. This average SD data is the SD forecast and then fed to the SCM for the final forecast.

Step-7: Input variables of the applied SD+SCM includes: (i) $\widehat{SD}_{t+1}$ (for 1-h ahead forecasting) or $\widehat{SD}_{t+1}$, $\widehat{SD}_{t+2}$, $\widehat{SD}_{t+3}$ (for 3-h-ahead forecasting); (ii) actual wind speed data, WS_t; (iii) actual wind direction data, WD_t, and (iv) actual temperature data, T_t.

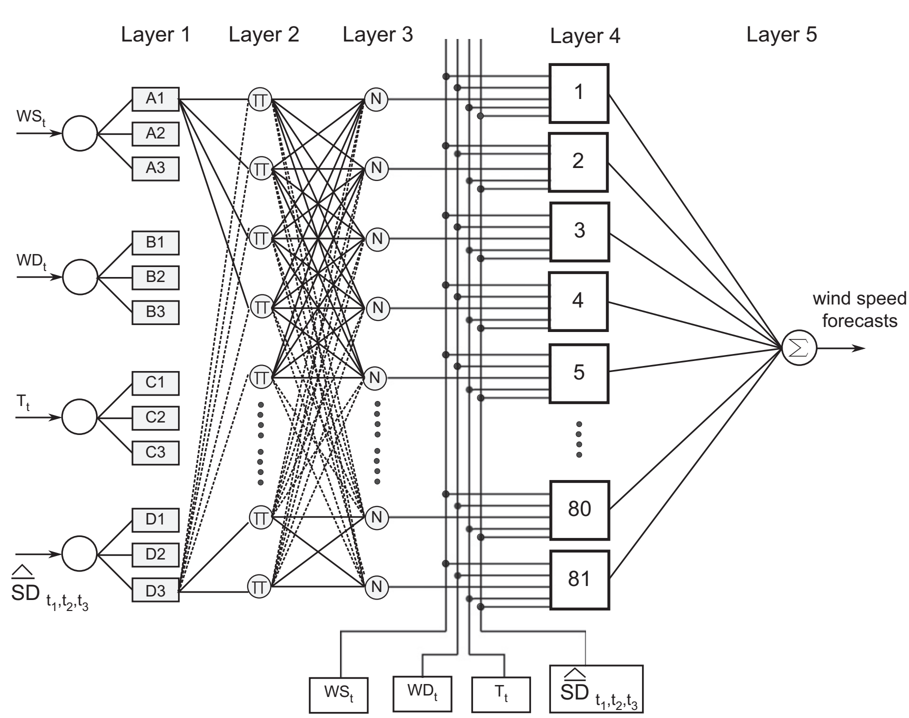


Fig. 6. Architecture of the ANFIS model for 3-h-ahead forecasting.

Table 1
Model parameter selection for SCMs.

Model	Parameters
BPNN	Learning rate (η) = 0.9, momentum (α) = 0.2, number of neurons in hidden layer = 9 (for 6 inputs), training function = TRAINLM, epoch = 1000
RBFNN	Spread of radial basis functions = 0.8, maximum number of neurons = 13, training function = "newrb" Matlab routine, epoch = 1000
ANFIS	Number of membership functions (μ) = 3, input/output membership function type = generalized bell-shaped, optimization method = HYBRID (combination of least-squares method and BP gradient descent method), epoch = 1000

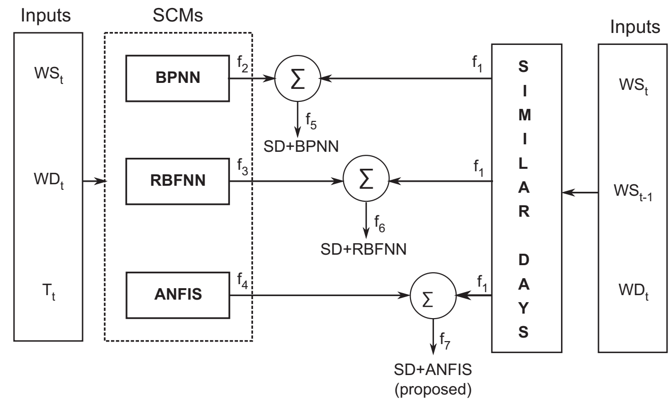


Fig. 7. Flow of wind speed forecasting using an integrated approach of similar days and soft computing model(s).

Step-8: This step involves the final forecasting of hourly wind speed using the combined SD+SCM. The input variables described in Step-7 are used in the trained SCM and we obtain the hourly wind speed forecasts.

With the change in forecast time, the initial conditions of the SCM parameters remain unchanged. If the forecast time is changed, SCM is retrained to obtain the relationship among WS, WD and T around the forecast day.

4. Numerical results and discussion

As stated previously, this paper presents a short-term wind speed forecasting technique based on averaging wind speed forecast of the SD method and refining the results through the application of SCMs. The forecasting approaches were tested using the real data of North Cape wind farm located in the PEI, Canada. Data sets of WS, WD and T are recorded in 10-min interval in the North Cape wind farm. The measured data of the six 10-min interval over an hour are averaged to obtain hourly data used in this paper. Given hourly wind speed forecasts are essential to have an effective output of the wind facilities and wind power production forecast. The power system operator requires hourly wind power production forecast in advance in order to carry out planning operations such as unit commitment and economic dispatch.

For a fair comparison, the same data and weather parameters are considered in all the forecasting models, i.e., SD, BPNN, RBFNN, ANFIS, SD+BPNN, SD+RBFNN, and SD+ANFIS. In a short form, SD+SCMs represent SD+BPNN, SD+RBFNN, and SD+ANFIS. The wind speed forecasting has been carried out using two major cases:

- Case-I: forecasting horizon considering 1-h-ahead, i.e., forecasting wind speed one hour before real-time for two different forecasting look-ahead times of 24 h (daily forecasts) and 72 h (three-day forecasts)
- Case-II: forecasting horizon considering 3-h-ahead, i.e., forecasting wind speed three hours before real-time for two different forecasting look-ahead times of 24 h (daily forecasts) and 72 h (three-day forecasts).

It is emphasized that cases-I and -II are carried out by randomly choosing one day (daily forecasts) and three continuous days (three-day forecasts) from each of the seasons of the year 2010. The actual flow of the wind speed forecasting process using SD and SCMs is shown in Fig. 7 where f_1, f_2, f_3, f_4, f_5, f_6, and f_7 represent forecast from the SD method, BPNN, RBFNN, ANFIS, SD+BPNN, SD+RBFNN, and SD+ANFIS models, respectively.

4.1. Accuracy measures

For all the days under study, three types of accuracy measures are computed to evaluate the performance of the forecasting models. The criteria to compare the performance of the proposed SD and SCMs are:

$$MAPE_{day} = \frac{1}{24}\sum_{i=1}^{24}\frac{|WS_i^{true} - WS_i^{forecast}|}{WS_i^{true}} * 100\%, \quad (8)$$

where $MAPE_{day}$ is the daily forecast error, WS_i^{true} is the actual wind speed in hour i, $WS_i^{forecast}$ is the predicted wind speed for that hour.

Analogous to the daily error, the three-day forecast error is computed as

$$MAPE_{three\text{-}day} = \frac{1}{72}\sum_{i=1}^{72}\frac{|WS_i^{true} - WS_i^{forecast}|}{WS_i^{true}} * 100\%. \quad (9)$$

Additionally, the root mean square error (RMSE) is also computed. This parameter is defined as the square root of the average of either 24 (daily) or the 72 (three-day) square differences between the predicted values and the true ones.

$$RMSE_{day} = \sqrt{\frac{1}{24}\sum_{i=1}^{24}(WS_i^{true} - WS_i^{forecast})^2}, \quad (10)$$

$$RMSE_{three-day} = \sqrt{\frac{1}{72}\sum_{i=1}^{72}(WS_i^{true} - WS_i^{forecast})^2}. \quad (11)$$

Furthermore, in order to assess the prediction capacity of the forecasting models, mean absolute error (MAE), which provides an indication of error ranges is calculated.

$$MAE = \frac{1}{M}\sum_{i=1}^{M}|WS_i^{true} - WS_i^{forecast}|, \quad (12)$$

where the value of M is 24 and 72 for daily and three-day forecasting, respectively.

4.2. 1-h-ahead wind speed forecasting results

Table 2 presents the case-I results obtained from all the chosen forecasting models and the results are compared with the persistence method. As seen from Table 2, the MAPE values obtained from the persistence method are 13.23%, 18.69%, 16.91%, and 6.75% for winter, spring, summer and fall, respectively. Note that December 20 (Monday), May 21 (Friday), July 5 (Monday) and October 10 (Sunday) of the year 2010 have been chosen from the seasons–winter, spring,

Table 2
Comparison of 1-h-ahead forecasting performance of the chosen models for the forecasting horizon of 24 h.

Season	Error	Persis	SD	BPNN	RBFNN	ANFIS	f_5	f_6	f_7^*
Winter	MAPE	13.23	14.82	13.88	13.67	12.85	8.89	8.67	7.65
	MAE	1.11	1.32	1.21	1.19	1.15	0.77	0.68	0.58
	RMSE	1.38	1.74	1.36	1.43	1.34	0.98	1.02	0.73
Spring	MAPE	18.69	13.72	15.82	14.11	13.88	10.88	9.23	8.02
	MAE	0.93	0.52	0.62	0.50	0.56	0.45	0.34	0.35
	RMSE	1.21	0.66	0.74	0.71	0.79	0.54	0.59	0.58
Summer	MAPE	16.91	9.52	14.37	13.92	14.13	9.45	9.65	7.27
	MAE	1.01	0.84	1.28	1.13	1.19	0.99	0.97	0.68
	RMSE	1.34	1.16	1.58	1.45	1.38	1.25	1.28	0.97
Fall	MAPE	6.75	8.72	11.75	10.36	11.06	6.85	7.46	6.17
	MAE	0.92	0.82	1.02	0.98	0.91	0.87	0.89	0.65
	RMSE	1.17	1.22	1.4	1.25	1.32	1.2	1.35	0.94

Persis: persistence method; f_5: SD+BPNN; f_6: SD+RBFNN; f_7^*: proposed SD+ANFIS model.

summer and fall, respectively. The MAPE values obtained from the SD, BPNN, RBFNN and ANFIS models in all the seasons show inconsistent results, i.e., these models are found to perform sometimes better than the persistence method in one season and worse in others. In winter, only the ANFIS model (12.85%) shows better performance than the other models over the persistence method (13.23%). However, the persistence method performs poorer in comparison to the SD, BPNN, RBFNN, and ANFIS models in both the spring and summer seasons. In fall, the MAPE values from all these single models are in the range of around 8%–11% and do not do as well as the persistence method (6.75%). From these results, it is observed that the performances of the considered SCMs and the SD method are seasonal sensitive and they produce inconsistent forecasting results.

In order to cope with the fluctuated performances of the SCMs and SD, this paper presents an integrated model that combines the SD method with the SCM, i.e., SD+SCM. With the application of SD+SCM, the errors are greatly improved as it can be observed in Table 2 that when SD is combined with ANFIS, the MAPE value is found to be lower (7.65%) than that of single use of SD (14.82%) and ANFIS (12.85%) in winter. So, with an introduction of SD into ANFIS model, the SD+ANFIS output resulted into an improvement in error by 40.46% over the ANFIS model. The MAPE values obtained from the SD+ANFIS demonstrate that there is a large improvement in error approximately in the range of 40%–48% in all the seasons over the direct use of ANFIS model only. An improvement in error from the SD+RBFNN and SD+BPNN models is found to be in the range of around 27%–36% and 31%–41% over the single use of RBFNN and BPNN, respectively.

The histogram as shown in Fig. 8 compares the MAPE values for 1-h-ahead forecasting. Note that Fig. 8 excludes the MAPE values obtained from BPNN, RBFNN, SD+BPNN and SD+RBFNN models as the focus here is to compare the MAPE obtained from the proposed SD+ANFIS model with the persistence, SD and ANFIS, and to illustrate a significant improvement in error when the ANFIS model is combined with the SD method compared to a single use of ANFIS model.

In order to demonstrate the prediction capabilities of the considered models, Table 2 also presents MAE and RMSE values for all the test cases. It is observed that the MAE and RMSE errors of low values are obtained from the SD+SCM models. In all the test cases, the SD method when combined with the SCM outperforms the direct use of a single SCM and compare favorably well over the persistence method. The results obtained from the proposed SD+ANFIS demonstrates the higher accuracy and

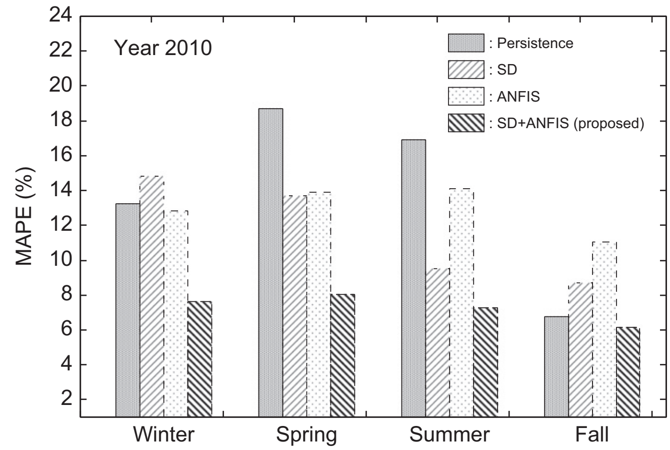


Fig. 8. 1-h-ahead errors for forecasting horizon of 24 h.

Table 3
Comparison of 1-h-ahead forecasting performance of the chosen models for the forecasting horizon of 72 h.

Season	Error	Persis	SD	BPNN	RBFNN	ANFIS	f_5	f_6	f_7^*
Winter	MAPE	15.21	15.58	13.65	14.55	14.80	10.11	10.55	9.87
	MAE	1.09	1.23	1.16	1.21	1.28	0.92	0.98	0.84
	RMSE	1.52	1.79	1.64	1.6	1.53	0.96	1.35	0.91
Spring	MAPE	22.79	25.69	18.54	17.13	15.67	12.13	12.14	10.1
	MAE	1.10	1.19	1.01	0.82	0.80	0.57	0.45	0.48
	RMSE	1.37	1.33	1.31	0.90	0.97	0.86	0.71	0.61
Summer	MAPE	11.73	11.41	15.01	14.93	13.86	12.28	11.3	9.11
	MAE	0.8	0.97	1.24	1.02	1.01	0.85	0.73	0.56
	RMSE	1.00	1.28	1.52	1.42	1.12	0.98	0.83	0.69
Fall	MAPE	21.08	12.05	14.86	11.77	11.89	12.25	10.71	9.78
	MAE	1.05	1.07	1.29	1.14	1.10	1.11	1.08	0.84

Persis: persistence method; f_5: SD+BPNN; f_6: SD+RBFNN; f_7^*: proposed SD+ANFIS model.

adequacy of this forecasting model. The reason of using 24-h prediction by repeating 1-h predictions is to deliver 1-h-ahead forecast for the next 24 h. Power system operator requires different length of forecasting horizon for an operation of interconnected power systems. However, increase in forecasting horizon would result into increase in forecasting error.

This paper also reports the performance of the various techniques by increasing the forecasting horizon up to 72 h, i.e., three-day forecasts for 1-h-ahead wind speed forecasting. Table 3 presents the three-day-forecasts for the period December 11–13 (winter), May 17–19 (spring), July 24–26 (summer), and October 27–29 (fall). The MAPE values using the persistence method are obtained in the range of 11.73%–22.79% in all the seasons. As expected, the performance of the persistence method is found to be deteriorated for the three-day forecasts compared to the daily forecast in which the MAPE range was 6.75%–18.69% (Table 2). As it can be seen in Table 3, the MAPEs for the SD method, SCMs, and SD+SCMs are also found to be increased, but at a lower extent when compared to the persistence. The sample average of MAPEs obtained from the SD+BPNN and SD+RBFNN models for 1-h-ahead (daily forecast) are in the range of 6.85%–10.88% and 7.46%–9.65% for all the seasons, respectively. These figures increase to only 10.11%–12.25% and 10.71%–12.14%, respectively, for the three-day forecasts. Again in the case of increase in forecasting horizon, the performance of the proposed SD+ANFIS

Table 4
Comparison of 1-h-ahead monthly forecasting performance.

Model	Error	Month										
		Feb	Mar	Apr	May	Jun	Jul	Aug	Sep	Oct	Nov	Dec
LP	MAPE	21.38	40.73	28.92	31.33	36.08	27.46	26.81	24.19	20.65	19.93	17.82
	MAE	1.12	1.20	0.96	1.34	1.27	1.08	1.11	1.17	0.76	0.84	0.68
	RMSE	1.86	2.34	2.13	2.17	2.34	1.73	2.07	2.25	1.52	1.73	1.32
NWP	MAPE	38.52	49.68	36.52	38.73	39.82	32.09	33.5	37.99	29.55	31.18	26.22
	MAE	1.37	1.22	1.08	1.42	1.33	1.25	1.19	1.36	0.98	1.08	0.94
	RMSE	2.24	2.73	2.33	2.45	2.84	1.98	2.36	2.69	1.88	2.09	1.79
f_7^*	MAPE	15.12	31.85	19.95	21.65	25.20	18.92	20.28	15.76	13.38	13.8	13.26
	MAE	0.71	0.92	0.91	0.99	0.82	0.89	0.71	0.92	0.80	0.76	0.88
	RMSE	0.94	1.18	1.20	1.30	0.99	1.14	0.89	1.16	1.00	0.99	1.19

f_7^*: proposed SD+ANFIS model.

forecasting model is superior than the persistence method and the other models as well. As it can be seen that the MAPEs obtained from the SD+ANFIS for the three-day forecasts increase only by small values (9.11%–10.10%) when compared to that of daily forecast (6.17%–8.02%). Furthermore, the low values of MAE and RMSE are generated by the proposed SD+ANFIS model and the values are within 1 m/s except that the RMSE in fall season is 1.23 m/s.

Table 4 shows the two-week forecasts for the period of February 16–28, 2010 and monthly forecasts for the period of March–December 2010 using LP and NWP models, and the results are then compared with the proposed SD+ANFIS. As the total data set available in this paper is for the period of January 2009 to December 2010, the monthly forecasts for January 2010 and the forecasts for February 1–15, 2010 are not reported in this paper. The reason behind this is the SD technique considers the data of previous 45 days from the day before a forecast day, and 45 days before and after from the forecast day in the previous year for the selection of similar days. The LP model results presented in Table 4 are the forecasts using one-year LP model, the detail of which is available in [43]. The NWP model, which is known as physical model, results presented in Table 4 are the forecasted values obtained from Environment Canada (EC) that uses NWP models for their wind speed forecasts. In all the simulated cases as shown in Table 4, our proposed model based on SD+ANFIS shows better performance compared to that of LP and NWP models. Furthermore, to have better comparison, monthly MAPE values presented in Table 4 are illustrated in Fig. 9 where we can observe the larger values of average monthly MAPEs for LP (26.86%) and NWP (35.80%) models compared to our proposed model (19.02%). In addition, Fig. 9 also shows the comparison of LP, NWP and the proposed model by means of MAPE deviation.

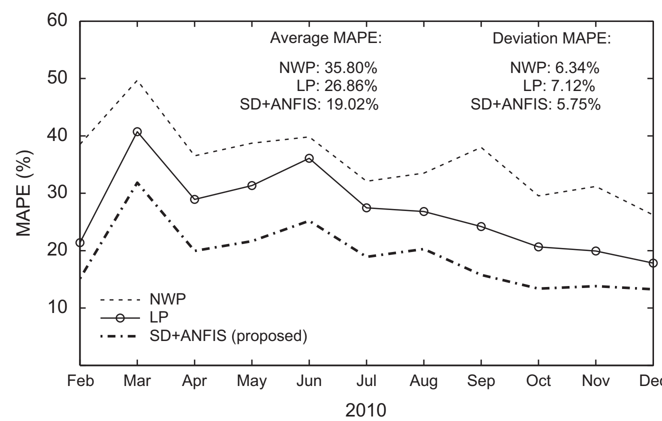


Fig. 9. 1-h-ahead MAPE monthly comparison.

4.3. 3-h-ahead wind speed forecasting results

In order to evaluate the prediction capability of the proposed SD+ANFIS model, this work also assesses 3-h-ahead forecasting (case-II results). In order to forecast and validate the performances of the SD+SCMs, the same days as chosen in case-I have been considered.

Table 5
Comparison of 3-h-ahead forecasting performance of the chosen models for the forecasting horizon of 24 h.

Season	Error	SD	BPNN	RBFNN	ANFIS	f_5	f_6	f_7^*
Winter	MAPE	20.91	16.12	15.91	14.9	10.53	10.91	9.23
	MAE	2.21	1.64	1.62	1.52	0.96	0.99	0.86
	RMSE	2.89	1.84	1.87	1.69	1.36	1.32	1.05
Spring	MAPE	22.22	20.09	19.23	19.86	14.08	12.00	10.77
	MAE	1.05	1.11	0.92	1.02	0.56	0.47	0.46
	RMSE	1.37	1.31	1.24	1.29	0.7	0.81	0.74
Summer	MAPE	14.21	19.62	18.87	20.17	12.35	11.23	10.34
	MAE	1.25	1.71	1.64	1.72	1.24	1.11	1.09
	RMSE	1.57	1.98	1.96	2.09	1.69	1.68	1.43
Fall	MAPE	13.12	18.29	18.76	17.94	11.52	11.79	10.36
	MAE	1.31	1.96	2.02	1.86	1.34	1.30	1.19
	RMSE	1.69	2.29	2.44	2.09	1.59	1.48	1.56

f_5: SD+BPNN; f_6: SD+RBFNN; f_7^*: proposed SD+ANFIS model.

Table 5 presents the MAPE results obtained from the SD, each SCM and combined SD+SCMs. The sample average daily MAPEs obtained from the SD method are 20.91%, 22.22%, 14.21%, and 13.12% for winter, spring, summer and fall, respectively. These figures increase to 22.52%, 26.11%, 18.10%, and 21.32% (Table 6) when the forecasting horizon is 72 h, respectively. As it can be observed in Table 5, the forecasting performances of BPNN, RBFNN and ANFIS models show inconsistency when compared with the SD method. It is seen that the BPNN, RBFNN and ANFIS models outperform the SD method in winter and spring, but fails to do so in the summer and fall. However, when SD is combined with the SCM, the forecasting performance is found to be enhanced. As it can be seen in Table 5, the MAPE value obtained from the proposed SD+ANFIS is lower (9.23%, 10.77%, 10.34% and 10.36%) than the single use of ANFIS (14.9%, 19.86%, 20.17% and 17.94%) in all the seasons. In other words, by combining SD and ANFIS, the SD+ANFIS output resulted in a

Table 6
Comparison of 3-h-ahead forecasting performance of the chosen models for the forecasting horizon of 72 h.

Season	Error	SD	BPNN	RBFNN	ANFIS	f_5	f_6	f_7^*
Winter	MAPE	22.52	21.95	20.10	19.97	17.12	15.92	14.88
	MAE	2.51	2.36	2.35	2.34	2.13	1.51	1.37
	RMSE	3.30	2.86	2.82	2.83	2.39	1.92	1.80
Spring	MAPE	26.11	25.94	23.22	22.14	16.88	13.88	13.31
	MAE	1.86	1.94	1.68	1.78	0.85	0.51	0.62
	RMSE	2.37	2.15	1.82	1.96	1.21	0.78	0.96
Summer	MAPE	18.1	24.00	20.46	20.36	17.23	15.53	13.84
	MAE	1.58	1.98	1.78	1.83	1.49	1.38	1.29
	RMSE	1.91	2.36	2.78	2.13	1.83	1.72	1.52
Fall	MAPE	21.32	22.82	20.26	18.83	17.79	15.26	14.94
	MAE	2.64	2.75	2.61	2.46	2.07	1.92	1.81
	RMSE	3.02	3.45	2.72	2.71	2.48	2.17	2.04

f_5: SD+BPNN; f_6: SD+RBFNN; f_7^*: proposed SD+ANFIS model.

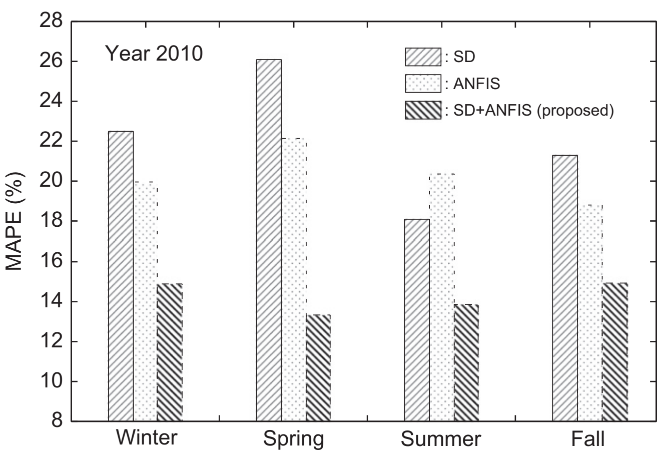


Fig. 10. 3-h-ahead errors for forecasting horizon of 72 h.

38.05%, 45.77%, 48.73% and 42.25% improvement in the MAPE values for winter, spring, summer and fall, respectively.

Table 6 presents 3-h-ahead forecasting results when the forecasting horizon is extended to 72 h. Note that in all the test cases as shown in Table 6, forecasting errors are significantly improved by the proposed SD+ANFIS model compared to the rest of the models. The performance of the proposed SD+ANFIS model in winter is such that its output (14.88%) resulted in a 25.48% improvement in the MAPE value over the single use of ANFIS (19.97%), and the percentage error improvements in spring, summer and fall are 39.88%, 32.02% and 20.65%, respectively. The histogram as shown in Fig. 10 for the three-day forecasts in all the seasons illustrates the comparison of MAPE value obtained from the proposed SD+ANFIS with the SD method and a single use of ANFIS model.

The values of maximum and minimum percentage error improvement obtained by using the SD+ANFIS model are 48.73% in summer (for 3-h-ahead forecasting when the forecasting horizon is 24 h) and 17.74% in fall (for 1-h-ahead forecasting when the forecasting horizon is 72 h). As demonstrated by the test results, it can be summarized that a significant improvement in forecasting wind speed errors are achieved from the proposed SD+ANFIS technique, providing accurate daily and three-day forecasts.

Table 7 shows errors comparison in the case of larger forecasting horizon. The MAPE values start deteriorating when the

Table 7
Performance of the proposed model in different forecasting horizons.

Season	Error	SD+ANFIS				
		1-h-ahead	3-h-ahead	6-h-ahead	12-h-ahead	24-h-ahead
Winter	MAPE	7.65	9.45	13.55	18.99	24.10
	MAE	0.58	0.98	1.53	1.74	1.76
	RMSE	0.73	1.23	1.94	2.19	2.07
Spring	MAPE	8.02	14.22	16.84	18.04	22.62
	MAE	0.35	0.87	1.83	1.96	1.85
	RMSE	0.58	1.04	2.14	2.26	2.31
Summer	MAPE	7.27	9.86	15.28	17.09	21.83
	MAE	0.68	0.89	1.76	1.91	1.94
	RMSE	0.85	0.96	1.86	2.13	2.22
Fall	MAPE	6.17	10.39	14.86	17.91	20.8
	MAE	0.65	0.82	1.55	1.86	1.89
	RMSE	0.82	0.93	1.73	1.97	2.40

forecasting horizon increases. This is due to the propagation of the error. In other words, as $\widehat{SD}_{t+1}$ increases, accumulated error that depends on forecasting period (hourly, daily, weekly, monthly, etc.) will also increase in case of predicting wind speed.

Forecasting short-term wind speed with a higher rate of accuracy is always a major concern for the power system operator. This paper contributes to alleviate the major problem of short-term wind speed forecasting in which the proposed prediction model based on ANFIS combined with the SD method is applied to forecast 1-h-ahead and 3-h-ahead wind speed. The average computation time required by the proposed hybrid SD+ANFIS model for 1-h-ahead daily wind speed forecasts is around 1 min using MATLAB on a PC with 4 GB of RAM and a 2.7-GHz-based processor.

5. Conclusions

This paper presented soft computing approaches for predicting short-term wind speed. The performances of the BPNN, RBFNN and ANFIS models were assessed with and without integration of the SD method. Wind speed forecasts are carried out in two different forms: (i) 1-h-ahead forecast, and (ii) 3-h-ahead forecast, both considering the forecasting horizon of 24 and 72 h. The interaction between wind speed and other weather parameters such as wind direction and temperature were taken into consideration in the wind speed forecast process. The test results obtained for 1-h-ahead and 3-h-ahead forecasts confirm that the proposed wind speed forecasting algorithm based on ANFIS combined with the SD method is capable of transforming the historical numerical weather data into wind speed predictions with higher accuracy. Possible future work would be to consider other weather variables such as humidity, pressure in order to generate wind speed and develop a model for the transformation of wind speed to wind power.

Acknowledgments

The authors are thankful to Wind Energy Institute of Canada (WEICan) and EC for providing the numerical weather data and wind forecast data, respectively, in order to carry out this research.

References

[1] Singh S, Erlich I. Strategies for wind power trading in competitive electricity markets. IEEE Transactions on Energy Conversion 2008;23(1):249–56.
[2] Georgilakis PS. Technical challenges associated with the integration of wind power into power systems. Renewable and Sustainable Energy Reviews 2008;12(3):852–63.
[3] Soman S, Zareipour H, Malik O, Mandal P. A review of wind power and wind speed forecasting methods with different time horizons. In: North American power symposium (NAPS); 2010. p. 1–8.
[4] Salcedo-Sanz S, Perez-Bellido AM, Ortiz-Garcia EG, Portilla- Figueras A, Prieto L, Paredes D. Hybridizing the fifth generation mesoscale model with artificial neural networks for short-term wind speed prediction. Renewable Energy 2009;34(6):1451–7.
[5] Ramirez-Rosado IJ, Fernandez-Jimenez LA, Monteiro C, Sousa J, Bessa R. Comparison of two new short-term wind-power forecasting systems. Renewable Energy 2009;34(7):1848–54.
[6] Wu Y-K, Hong J-S. A literature review of wind forecasting technology in the world. In: Power tech, 2007 IEEE Lausanne; 2007. p. 504–9.
[7] Kavasseri RG, Seetharaman K. Day-ahead wind speed forecasting using f-ARIMA models. Renewable Energy 2009;34(5):1388–93.
[8] Taylor J, McSharry P. Short-term load forecasting methods: an evaluation based on european data. IEEE Transactions on Power Systems 2007;22(4): 2213–9.
[9] Costa A, Crespo A, Navarro J, Lizcano G, Madsen H, Feitosa E. A review on the young history of the wind power short-term prediction. Renewable and Sustainable Energy Reviews 2008;12(6):1725–44.
[10] Shi J, Guo J, Zheng S. Evaluation of hybrid forecasting approaches for wind speed and power generation time series. Renewable and Sustainable Energy Reviews 2012;16(5):3471–80.
[11] Kariniotakis G, Stavrakakis G, Nogaret E. Wind power forecasting using advanced neural networks models. IEEE Transactions on Energy Conversion 1996;11(4):762–7.
[12] Kusiak A, Zheng H, Song Z. Short-term prediction of wind farm power: a data mining approach. IEEE Transactions on Energy Conversion 2009;24(1): 125–36.
[13] Mabel M, Fernandez E. Estimation of energy yield from wind farms using artificial neural networks. IEEE Transactions on Energy Conversion 2009;24(2): 459–64.
[14] Zhang L, Luh P. Neural network-based market clearing price prediction and confidence interval estimation with an improved extended kalman filter method. IEEE Transactions on Power Systems 2005;20(1):59–66.
[15] Amjady N, Daraeepour A, Keynia F. Day-ahead electricity price forecasting by modified relief algorithm and hybrid neural network. Generation, Transmission Distribution, IET 2010;4(3):432–44.
[16] Zhou J, Shi J, Li G. Fine tuning support vector machines for short-term wind speed forecasting. Energy Conversion and Management 2011;52(4):1990–8.
[17] Kartalopoulos SV. Understanding neural networks and fuzzy logic: basic concepts and applications. 1st ed.Wiley-IEEE Press; 1997.
[18] Bilgili M, Sahin B, Yasar A. Application of artificial neural networks for the wind speed prediction of target station using reference stations data. Renewable Energy 2007;32(14):2350–60.
[19] Tanuwijaya K, Chen S-M. A new method to forecast enrollments using fuzzy time series and clustering techniques. In: International conference on machine learning and cybernetics, 2009, vol. 5; 2009. pp. 3026–9.
[20] Damousis I, Alexiadis M, Theocharis J, Dokopoulos P. A fuzzy model for wind speed prediction and power generation in wind parks using spatial correlation. IEEE Transactions on Energy Conversion 2004;19(2):352–61.
[21] Haque AU, Meng J. Short-term wind speed forecasting based on fuzzy ARTMAP. International Journal of Green Energy 2011;8(1):65–80.
[22] Giorgi MGD, Ficarella A, Tarantino M. Error analysis of short term wind power prediction models. Applied Energy 2011;88(4):1298–311.
[23] Li G, Shi J, Zhou J. Bayesian adaptive combination of short-term wind speed forecasts from neural network models. Renewable Energy 2011;36(1):352–9.
[24] Cadenas E, Rivera W. Wind speed forecasting in three different regions of mexico, using a hybrid ARIMA–ANN model. Renewable Energy 2010;35(12): 2732–8.
[25] Blonbou R. Very short-term wind power forecasting with neural networks and adaptive Bayesian learning. Renewable Energy 2011;36(3):1118–24.
[26] Bhaskar K, Singh S. AWNN-assisted wind power forecasting using feed-forward neural network. IEEE Transactions on Sustainable Energy 2012;3(2): 306–15.
[27] Madsen H, Pinson P, Kariniotakis G, Nielsen HA, Nielsen TS. Standardizing the performance evaluation of short term wind power prediction models. Wind Engineering 2005;29(6):475–89.
[28] Madsen H. A protocol for standardizing the performance evaluation of short-term wind power prediction models, Project ANEMOS Deliverable 2.3; 2004.
[29] Giebel G, Brownsword R, Kariniotakis G, Denhard M, Draxl C. The state-of-the-art in short-term prediction of wind power: a literature overview, 2nd edition. ANEMOS.plus; 2011.
[30] Mandal P, Senjyu T, Urasaki N, Funabashi T, Srivastava A. A novel approach to forecast electricity price for pjm using neural network and similar days method. IEEE Transactions on Power Systems 2007;22(4):2058–65.
[31] Mandal P, Srivastava A, Park J-W. An effort to optimize similar days parameters for ANN-based electricity price forecasting. IEEE Transactions on Industry Applications 2009;45(5):1888–96.
[32] Mandal P, Srivastava AK, Negnevitsky M, Park J-W. Sensitivity analysis of neural network parameters to improve the performance of electricity price forecasting. International Journal of Energy Research 2009;33(1):38–51.
[33] Amanda MGG, Hering S. Powering up with space–time wind forecasting. Journal of the American Statistical Association 2010;105(489):92–104.
[34] Weisberg S. Applied Linear Regression, 3rd ed., vol. 528. John Wiley & Sons; 2005.
[35] Li G, Shi J. On comparing three artificial neural networks for wind speed forecasting. Applied Energy 2010;87(7):2313–20.
[36] Lei M, Shiyan L, Chuanwen J, Hongling L, Yan Z. A review on the forecasting of wind speed and generated power. Renewable and Sustainable Energy Reviews 2009;13(4):915–20.
[37] Negnevitsky M. Artificial intelligence: a guide to intelligent systems. 1st ed. Boston, MA, USA: Addison-Wesley Longman Publishing Co., Inc.; 2001.
[38] Sideratos G, Hatziargyriou ND. Application of radial basis function networks for wind power forecasting. In: International conference on artificial neural networks; 2006. p. 726–35.
[39] Yun Z, Quan Z, Caixin S, Shaolan L, Yuming L, Yang S. RBF neural network and ANFIS-based short-term load forecasting approach in real-time price environment. IEEE Transactions on Power Systems 2008;23(3):853–8.
[40] Jang J-S. ANFIS: adaptive-network-based fuzzy inference system. IEEE Transactions on Systems, Man and Cybernetics 1993;23(3):665–85.
[41] Catalao J, Pousinho H, Mendes V. Hybrid wavelet-PSO-ANFIS approach for short-term wind power forecasting in Portugal. IEEE Transactions on Sustainable Energy 2011;2(1):50–9.
[42] Potter C, Negnevitsky M. Very short-term wind forecasting for Tasmanian power generation. IEEE Transactions on Power Systems 2006;21(2):965–72.
[43] El-Fouly T, El-Saadany E, Salama M. One day ahead prediction of wind speed using annual trends. In: Power engineering society general meeting, 2006. IEEE; 2006. p. 726–35.